JOURNAL OF SOLID STATE CHEMISTRY 88, 140–162 (1990)

Layered Cuprates with Double and Triple Copper Layers: Structure and Superconductivity

B. RAVEAU, C. MICHEL, AND M. HERVIEU

Laboratoire CRISMAT, CNRS-ISMRA, Université de Caen, Campus 2, Boulevard du Maréchal Juin 14032, Caen Cédex, France

Received April 18, 1990

DEDICATED TO J. M. HONIG ON THE OCCASION OF HIS 65TH BIRTHDAY

Layered cuprates with double and triple copper layers appear as potential materials for superconductivity at high temperature. A review of their crystal structure in connection with their superconducting properties, ruling out the electron microscopy studies, is made here. The main issues include the nonsuperconductive layered cuprates of the "systems" $Sr_2LnCu_2O_{6-x}$–$Ln_2SrCu_2O_6$, the important role of oxygen nonstoichiometry in superconductivity for thallium cuprates, the oxygen inhomogeneity in lead cuprates, and the proximity effects in bismuth cuprates. © 1990 Academic Press, Inc.

Introduction

Systematic investigation of oxides containing copper has been carried out by many groups these last 4 years simultaneously. A large family of layered cuprates was isolated, with the general formula $(ACuO_{3-x})_m(A'O)_n$ noted $[m,n]$, corresponding to the intergrowth of multiple oxygen-deficient perovskite layers and multiple rock salt-type layers. A great number of those oxides exhibit superconducting properties at high temperature owing to the presence of the mixed valence of copper Cu(II)–Cu(III) and to the bidimensional character of their structure. Many reviews have been devoted to the structural principles and nonstoichiometry phenomena in connection with the superconducting properties of these materials. In the present paper, we would like to focus our attention on the oxides involving double (m = 2) and triple (m = 3) copper layers. Those oxides were indeed found to exhibit the highest critical temperatures up to now. Nevertheless, several issues concerning these materials did not receive any answer, and suggest that the relationships between crystal chemistry and superconductivity in those phases are more complex than expected in a first approach. About 20 compounds or solid–solutions involve double or triple copper layers as shown in Table I. A great number of them are superconductors. However, one can notice that, curiously, those which exhibit single rock salt layers do not superconduct. These materials will be the subject of the first part of this paper. The thallium cuprates appeared very early as potential materials with the highest T_c's, and it was thought that the value of the critical temperature was closely dependent on the number of copper layers in the perovskite slab. Recently, it was shown that the relationship between T_c's and oxygen nonstoichiometry is very complex. This issue will be exposed in the second part of this review. Besides these oxides, the lead cuprates which have been isolated recently represent promising mate-

0022-4596/90 $3.00

TABLE I
THE DIFFERENT LAYERED CUPRATES (A Cu $O_{3-x})_m$ $(A'O)_n$ WITH DOUBLE (m = 2) AND TRIPLE (m = 3) COPPER LAYERS

m = 2: $(ACuO_{3-x})_2$ $(A'O)_n$		m = 3: $(A'CuO_{3-x})_3$ $(A'O)_n$	
		n = 1	
$La_{2-x}Sr_{1+x}Cu_2O_6$ (*1, 3*)	N.S.C.	$PbBaYSrCu_3O_8$ (*11*)	N.S.C.
$La_{2-x}Ca_{1+x}Cu_2O_6$ (*2*)	N.S.C.	$PbBaYSr_{1-x}Ca_xCu_3O_8$ (*11*)	S.C.(?)
$A_{2-x}Ln_{1+x}Cu_2O_{6-y}$ (*5, 6*)	N.S.C.		
$Sr_2NdCu_2O_{5.76}$ (*10*)	N.S.C.		
$Sr_{1-9}La_{1.1}Cu_2O_{5.83}$ (*9*)	N.S.C.		
$Sr_6Nd_3Cu_6O_{17}$ (*7*)	N.S.C.		
		n = 2	
$TlBa_2CaCu_2O_7$ (*16, 17*)	S.C.	$Tl\ Ba_2Ca_2Cu_3O_9$ (*27–29*)	S.C.
$TlSr_2CaCu_2O_7$ (*20*)	S.C.	$Tl_{0.5}Pb_{0.5}Sr_2Ca_2Cu_3O_9$ (*19*)	S.C.
$Tl_{0.5}Pb_{0.5}Sr_2CaCu_2O_7$ (*19*)	S.C.		
$TlBa_2LnCu_2O_7$ (*22*) (Ln = Y,Nd)	N.S.C.		
$Tl\ Ba_2Ca_{1-x}Cu_2O_7$ (*23, 24*)	S.C.		
(Tl,Bi) $Sr_2Ca_{1-x}Y_xCu_2O_7$ (*25, 26*)	S.C.		
$Pb_{0.5}Sr_{2.50}Y_{1-x}Ca_xCu_2O_7$ (*50, 51*)	S.C.		
$Pb_{0.5}Ca_{0.5}Sr_2Y_{1-x}Ca_xCu_2O_7$ (*52*)	S.C.		
		n = 3	
$Tl_2Ba_2Ca\ Cu_2O_8$ (*32–36*)	S.C.	$Tl_2Ba_2Ca_3Cu_3O_{10}$ (*32, 34, 35, 39*)	S.C.
$Tl_2Ba_{2-x}Sr_xCaCu_2O_8$ (*37*)	S.C.	$Bi_2Sr_2Ca_2Cu_3O_{10}$ (*66–71*)	S.C.
$Bi_2Sr_2CaCu_2O_8$ (*55–63*)	S.C.	$Bi_{2-x}Pb_xSr_{2-x}Ca_{2+x}Cu_3O_{10}$ (*67*)	S.C.
$Bi_{2-x}Pb_xSr_2Ca_{1-x}Ln_xCu_2O_8$ (*64*)	S.C.		
$Tl_{2-x/3}Ba_{1+x}Tl_{1-x}LnCu_2O_8$ (*38*)	N.S.C.		

rials for superconductivity. Nevertheless, they generally exhibit broad resistive transitions. This third point will be discussed here. Although they exhibit high T_c, the bismuth cuprates are characterized by strong reversibility effects under a magnetic field. The problems of incommensurability and proximity effects in those latter phases will be discussed in the last part of this paper.

I. Nonsuperconductive Cuprates with Single Rock Salt-Type Layers

The oxides $La_{2-x}A_{1+x}Cu_2O_{6-x/2+\delta}$ (A = Ca,Sr) were the first layered cuprates of the family $(ACuO_{3-x})_m(A'O)_n$ which were synthesized (*1*). They crystallize in the tetragonal system ($a \approx a_p$, $c \sim 20$ Å). Their structure which was recently confirmed by neutron diffraction in the case of calcium (*2*) and strontium (*3*) corresponds to m = 2 and n = 1, i.e., consists of double pyramidal copper layers interleaved with calcium or strontium cations and intergrown with single rock salt-type layers (Fig. 1). The electron transport properties of these materials were also investigated 10 years ago in the range 100–300 K (*4*). They show a progressive evolution from a semiconducting to a semimetallic behavior (Fig. 2) as the trivalent copper content increases. The Seebeck effect measurements evidenced also a hole conduction (Fig. 3). It is remarkable that these oxides do not exhibit any supercon-

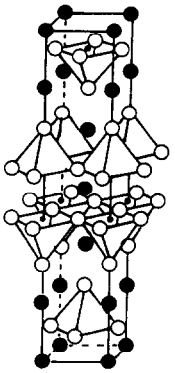

FIG. 1. Structure of the oxide $La_{1.9}Sr_{1.1}Cu_2O_6$: La,Sr (large solid circles), Cu (small solid circles), O (open circles).

ductivity in spite of their lamellar structure characterized by double copper layers absolutely similar to those observed in thallium and bismuth cuprates and of the existence of the mixed valency Cu(II)–Cu(III).

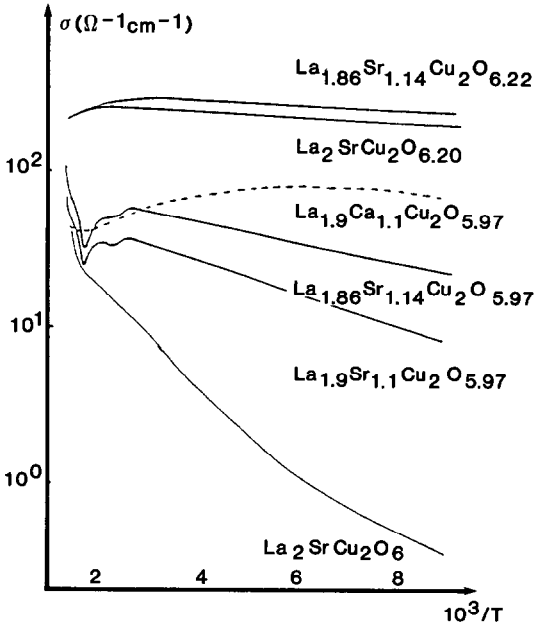

FIG. 2. Conductivity σ (logarithmic scale) vs reciprocal temperature for various compositions in the series $La_{2-x}A_{1+x}Cu_2O_{6-x/2+\delta}$.

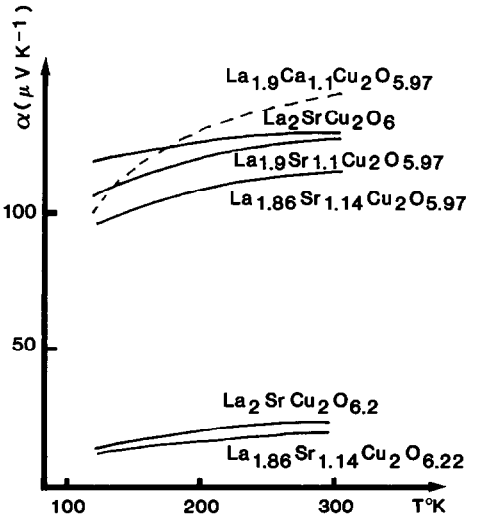

FIG. 3. Seebeck coefficient α plotted as a function of absolute temperature for $La_{2-x}A_{1+x}Cu_2O_{6-x/2+\delta}$.

The oxygen nonstoichiometry in those oxides is rather complex, due to the possible intercalation of excess oxygen between pyramidal layers, leading to formulations of the type $La_{2-x}A_{1+x}Cu_2O_{6+y}$ by annealing under an oxygen flow. The reversibility of this phenomenon and its dramatic influence on the conductivity is shown in Fig. 4 for $La_{1.9}Ca_{1.10}Cu_2O_{6-x}$. It can be seen that starting from the oxide "$x = 0.04$," which exhibits a semimetallic behavior, and heating under argon lead to a drastic decrease of conductivity due to a departure of oxygen as soon as the temperature reaches 373 K; if one stops the heating at 570 K and cools the sample down to 100 K, a semiconducting behavior is observed, which is also obtained by heating again the sample in the same inert atmosphere up to 570 K. Stopping heating at this temperature and introducing air lead immediately to an abrupt increase of the conductivity due to the very fast absorption of oxygen by the sample. These properties of intercalation–disintercalation of oxygen must be emphasized since they can be used advantageously to day to adjust the number

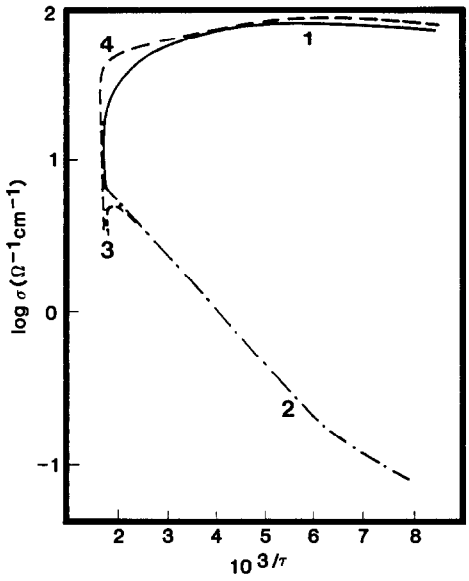

FIG. 4. Conductivity σ (logarithmic scale) vs $10^3/T$ under different atmospheres for the $La_{1.90}Ca_{1.10}Cu_2O_{5.97}$ compound: (1) first heating under inert atmosphere, (2) first cooling then second heating under inert atmosphere, (3) air introduction at high temperature, (4) cooling in air.

of hole carriers in the thallium cuprates and consequently to optimize their superconducting properties as will be shown below.

Besides, this first class of [2, 1]-layered cuprates, a second series of oxides, with richer strontium contents, were isolated (*5*). These oxides, which correspond always to the general formula $Ln_{2-x}Sr_{1+x}Cu_2O_{6-x/2+\delta'}$, differ from the lanthanide-rich oxides by a significant deficiency with respect to the "O_6" ideal formula given above. They were obtained for samarium, europium, and gadolinium with x values ranging from 0.70 to 0.90. Recently, a similar phase was synthesized for lanthanum (*6*). The crystallographic characteristics of those oxides which are given in Table II show that they differ from the preceding oxides by a tripling of one of the parameters leading to an orthorhombic cell with $a \approx a_p$, $b \approx 3a_p$,

TABLE II

CELL PARAMETERS OF THE ORTHORHOMBIC OXIDES $Ln_{2-x}Sr_{1+x}Cu_2O_{6-x/2+\delta}$ (Ln = Sm, Eu, Gd)

Ln	Composition	*x*	*a*(Å)	*b*(Å)	*c*(Å)	*V*(Å³)
Sm	$Sm_{1.3}Sr_{1.7}Cu_2O_{5.65}$	0.7	3.746	11.416	20.068	858.2
	$Sm_{1.1}Sr_{1.9}Cu_2O_{5.5}$	0.9	3.747	11.439	20.058	859.7
Eu	$Eu_{1.4}Sr_{1.6}Cu_2O_{5.70}$	0.6	3.742	11.325	20.052	849.8
	$Eu_{1.3}Sr_{1.7}Cu_2O_{5.65}$	0.7	3.744	11.337	20.047	850.9
	$Eu_{1.1}Sr_{1.9}Cu_2O_{5.55}$	0.9	3.742	11.380	20.020	852.5
Gd	$Gd_{1.3}Sr_{1.7}Cu_2O_{5.65}$	0.7	3.738	11.350	20.045	850.4
	$Gd_{1.1}Sr_{1.9}Cu_2O_{5.55}$	0.9	3.739	11.385	20.015	851.8

$c \approx 20$ Å ($a_p \approx 3.8$ Å, cell parameter of the cubic perovskite cell).

Recently, a new layered cuprate $Sr_6Nd_3Cu_6O_{17}$ was synthesized by solid state reaction under an argon flow and its structure was determined by neutron diffraction (*7*). This phase, which can also be formulated $Sr_2NdCu_2O_{5.66}$, exhibits similar parameters to those observed for the other strontium-rich compounds. The structure of this oxide (Fig. 5) is characterized by a similar arrangement of the metallic atoms and a great part of the oxygen atoms with respect to the $La_2SrCu_2O_6$-type structure (Fig. 1). However, several of the oxygen atoms and an-

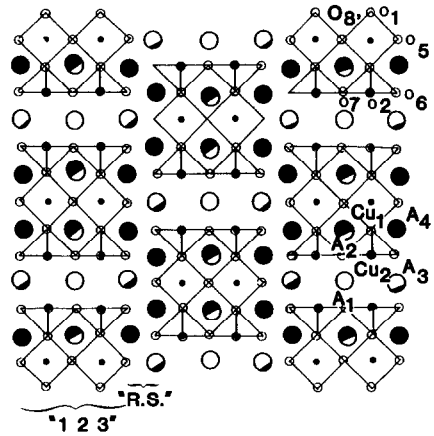

FIG. 5. Schematic drawing of the structure of the oxide $Sr_6Nd_3Cu_6O_{17}$.

ionic vacancies are distributed in a different way. Consequently, it appears that this structure is intermediate between the structure of the "123" phase $YBa_2Cu_3O_7$ (*8*) and the "0212" structure of $La_2SrCu_2O_6$. One can describe it as a regular intergrowth of the "123"-type structure with the rock salt structure. It is indeed built up from "123"-type ribbons $[Sr_{7/6}Nd_{5/6}Cu_2O_{4.66}]_\infty$ running along $\vec{b}$ and from $[Sr_{5/6}Nd_{1/6}O]_\infty$ rock salt-type layers parallel to (100). Thus $Sr_6Nd_3Cu_6O_{17}$ can be considered as the member $m = 2$, $n = 1$ of a series of intergrowths of general formula $[ACuO_{2.33}]_m^{\text{"123"}}[AO]_n^{rs}$, in which A will correspond to an adequate content of alkaline earth cations (Sr, Ba) and of lanthanides. The "123" $[Sr_{7/6}Nd_{5/6}Cu_2O_{4.66}]_\infty$ ribbons, which are three polyhedra wide along $\vec{b}$ ($2CuO_5 + 1\ CuO_4$) exhibit a significant difference with the classical $YBa_2Cu_3O_7$ structure (*8*). The Cu–O interatomic distances show indeed that the CuO_4 groups as the CuO_5 pyramids are strongly distorted with Cu–O distances ranging from 1.85 to 2.22 Å. The apical Cu–O distance of the CuO_5 pyramid (2.22 Å) is shorter than that observed for $YBa_2Cu_3O_7$ (2.29 Å), whereas a large distortion is observed in the basal plane (1.88 to 2.02 Å) compared to $YBa_2Cu_3O_7$ (1.93 to 1.96). The CuO_4 groups are no more planar; Cu(1), two O(1) atoms, and O(5) remain approximately in the same plane whereas O(8′), which ensures the junction between two CuO_4 groups, is significantly out of this plane leading to a Cu–O–Cu angle of 110° instead of 180°. Those features are easily understable if one considers the sequence of "123" ribbons along $\vec{c}$ (Fig. 5). Two successive ribbons are indeed shifted of about 3.8 Å along $\vec{b}$, so that at a same level along this latter direction, a neodymium plane is replaced by a copper plane. Such an arrangement induces strains in the structure which can only be decreased by a distortion of the CuO_4 and CuO_5 polyhedra and by their tilting.

The distribution of the strontium and neodymium cations is remarkable and is certainly an important factor for the stabilization of such a structure. One indeed observes that in the middle of the "123"-type ribbons the smaller cations, neodymium, take the place of yttrium in eight-fold coordination (Nd(1) sites) whereas, in the rock salt-type layers, the sites which exhibit an sixfold coordination (Sr(4) sites) are only occupied by strontium. On the opposite, the cationic sites which are located at the intersection of the rock salt layer and of the basal planes of the CuO_5 pyramids (Nd/Sr(3) sites) are occupied half by strontium and half by neodymium. In the same way, it is worth pointing out that the barium sites, in the "123" ribbons, are occupied by much smaller cations, half neodymium and half strontium (Nd/Sr (2) sites). This latter occupancy may be at the origin of the distortion of the CuO_4 square groups and may allow an adjustment of the "123" and rock salt layers.

The structure of the other strontium-rich compounds, with oxygen contents intermediate between "$O_{5.66}$" and "O_6", is up to now not completely elucidated. Nevertheless, the neutron diffraction studies of the oxides $La_{1.1}Sr_{1.9}Cu_2O_{5.83}$ (*9*) and $NdSr_2Cu_2O_{5.76}$ (*10*) clearly show that their structure is closely related to that of $Sr_6Nd_3Cu_3O_{17}$. The oxygen distribution in the structure can indeed be interpreted as the result of the intimate intergrowth of two extreme structures, the first one corresponding to $Sr_6Nd_3Cu_3O_{17}$ (Fig. 5) and the second one corresponding to the hypothetical compound $Sr_2NdCu_2O_6$ whose ideal structure (Fig. 6) would consist of six-sided tunnels built up from rings of six corner-sharing CuO_5 pyramids. Such tubes would be arranged in such a way that they form fluorite-type cages, and rock salt-type layers where the Nd and Sr cations are located.

From all these results it is clear that the oxygen nonstoichiometry in the "0212" oxides is far not completely understood and

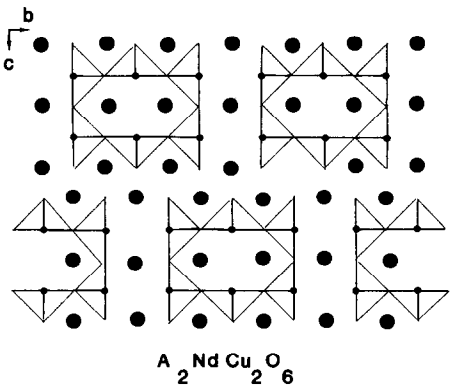

FIG. 6. Schematic drawing of the structure of the hypothetical oxide $Sr_2NdCu_2O_6$.

that it should be possible to synthesize new phases by playing with ordering of oxygen and vacancies, i.e., by changing the thermal treatments (temperature, time) and also the nature of the gaseous atmosphere. Although they do not superconduct, the knowledge of their magnetic and electron transport properties will be of capital importance in order to understand superconductivity in layered cuprates.

Another layered cuprate $PbBaYSrCu_3O_8$ (*11*) involving single rock salt layers has been recently isolated. This oxide represents the [3,1] member of the $(ACuO_{3-x})_m(A'O)_n$ family. Its structure (Fig. 7) consists of triple copper layers ($m = 3$) with copper in pyramidal and square planar coordination forming fluorite-type cages where strontium and yttrium are located. These oxygen-deficient perovskite layers are intergrown in the single rock salt-type layers containing mainly lead and barium. Assuming that a great part of lead exhibits the divalent state since located on the same site as barium, it can be seen that the two factors required for superconductivity—mixed valency of copper and low dimensionality of the structure—are obtained for this compound. Again, as for the other phases involving single rock salt-type layers, no superconductivity was detected. Nevertheless, it should be pointed out that a partial substitution of calcium for strontium led to a phase in which approximately 1% diamagnetism was detected at 50 K. Unfortunately, it could not be proved whether such a phenomenon was not due to traces of other superconductive lead cuprates.

As a conclusion, it is remarkable that the La_2CuO_4-type oxides remain the only oxides with single rock salt-type layers (*12*) which exhibit up-to-date superconducting properties (*13*).

II. Thallium Cuprates: The Spectacular Effect of Oxygen Nonstoichiometry upon T_c

After the discovery of superconductivity at 85–100 K in the system Tl–Ba–Ca–Cu–O (*14, 15*) a great number of superconductive thallium cuprates were isolated by different authors. Among those oxides, the compounds which appear as most promising are those which exhibit double and triple copper layers, owing to the fact that they exhibit the highest T_c's and that they seem more stable than the other thallium cuprates of the series. Nine oxides: [2,2] [3,2], [2,3], and [3,3] members of the series $(ACuO_{3-x})_m$

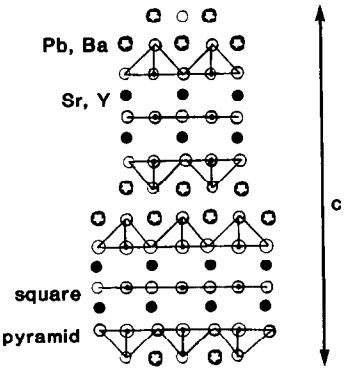

FIG. 7. Idealized drawing of the "0223" structure: $PbBaYSrCu_3O_8$.

$(A'O)_n$ are known up to now. Seven of them are superconductors. These materials can be subdivided into two series according to their structure. The [2,2] and [2,3] members correspond to the first series with formula $TlA_2Ca_{m-1}Cu_mO_{2m+3}$ and are characterized by double rock salt-type layers involving thallium monolayers (Figs. 8a and 8b). The [3,2] and [3,3] members belong to the second series $Tl_2A_2Ca_{m-1}Cu_mO_{2m+4}$ (Figs. 8c and 8d), involving triple rock salt layers, i.e., thallium bilayers.

The "1212"-phases, corresponding to the intergrowth of double pyramid layers with double rock salt layers (Fig. 8a), exhibit a wide range for critical temperatures, de-

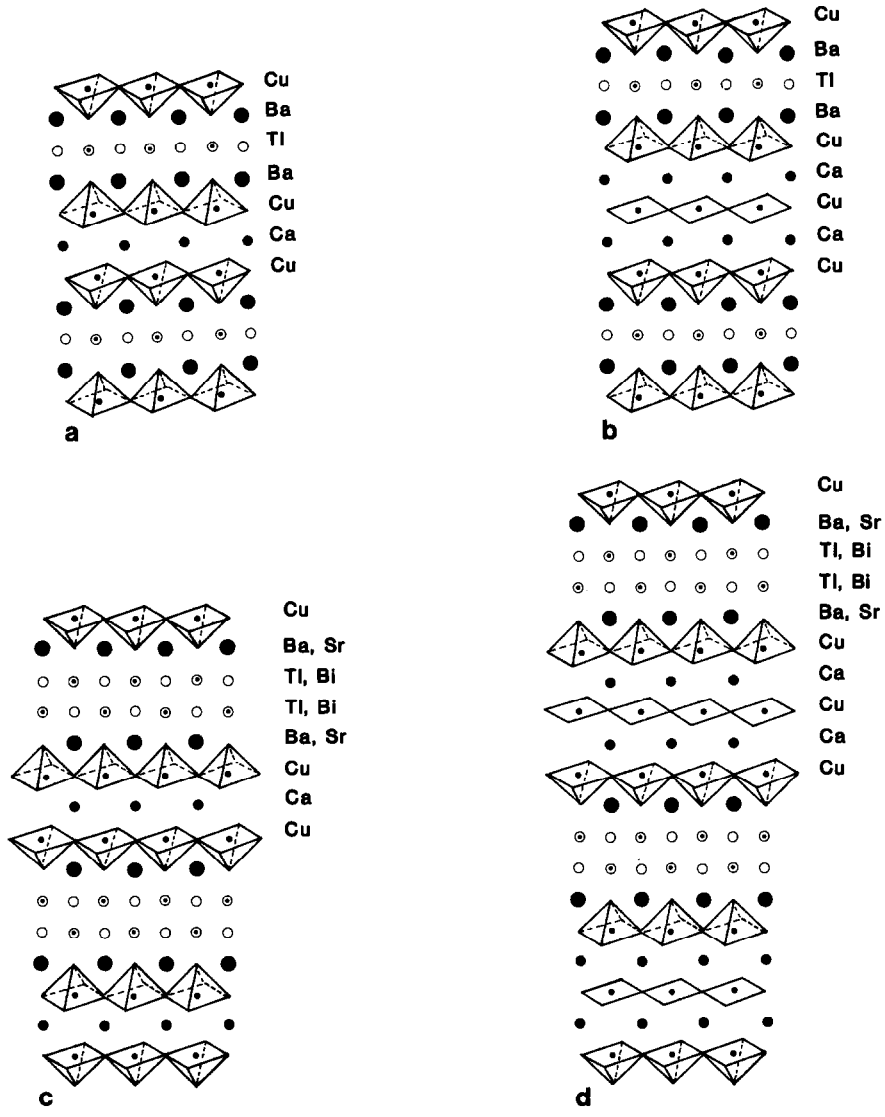

FIG. 8. Schematized structures of (a) "1212" oxides, e.g., $TlBa_2CaCu_2O_7$ ($m = 2$, $n = 2$); (b) "1223" oxides, e.g., $TlBa_2Ca_2Cu_3O_{10}$ ($m = 3$, $n = 2$); (c) "2212" oxides, e.g., $Tl_2Ba_2CaCu_2O_8$ or $Bi_2Sr_2CaCu_2O_8$ ($m = 2$, $n = 3$); and (d) "2223" oxides, e.g., $Tl_2Ba_2Ca_2Cu_3O_{10}$ or $Bi_2Sr_2Ca_2Cu_3O_{10}$ ($m = 3$, $n = 3$).

pending on the nature of the oxide, but also on the experimental method. Moreover, the synthesis of some of them is sometimes very difficult owing to the formation of intergrowths corresponding to other members of the family. $TlBa_2CaCu_2O_7$ was discovered by two staffs almost simultaneously (*16, 17*). The critical temperature of this phase was found to be variable according to the authors, ranging from 50 K (*17*) to100–112 K (*16, 18*). Moreover it was observed by the different authors that it was very difficult to obtain for this compound a high purity, leading very often to the existence, besides that phase, of intergrowths corresponding to other members of the series. The synthesis of the corresponding strontium oxide $TlSr_2CaCu_2O_7$ is still much more difficult. Several attempts made by Subramanian *et al.* (*19*) were unsuccessfull, whereas Martin *et al.* (*20*) prepared it as a mixture containing a majority of $TlSr_2CaCu_2O_7$ (about 90%) and observed superconducting properties with zero resistance below 47 K, and a diamagnetic volume fonction of 13%. The "1212" structure can be stabilized in a very attractive manner by substituting lead for thallium leading to the original phase $Tl_{0.5}Pb_{0.5}Sr_2CaCu_2O_7$, isolated by Subramanian *et al.* (*19*). The latter authors showed that the critical temperature of this phase was stabilized at 85 K. Its structure (Fig. 8a) is derived from the pure thallium oxides by replacing half of the thallium cations by lead in the thallium monolayers. It is worth pointing out that the Pb–O distances (*19*) as well as the X-ray absorption study (*21*) suggest that in this phase lead exhibits the tetravalent state. The complete substitution of calcium by a trivalent rare earth element, such as yttrium or neodymium, is possible without changing the structure, but kills the superconducting properties as shown for the oxides $TlBa_2Ln Cu_2O_7$ (*22, 23*). On the other hand, the partial substitution of calcium by such a lanthanide enhances the critical temperature. For instance, an increase of T_c from 73 to 103 K was observed for the oxide $TlBa_2Ca_{1-x}Y_x Cu_2O_7$ as x increases from 0 to 0.2 (*24*); however, Meissner fraction extrapolated at 0 K decreases drastically at the same time from 46% in the nondoped sample to 0.2% for $x = 0.20$. In the same way, superconductivity in the region 60–90 K was found for the oxides $TlSr_2Ca_{1-x}Ln_xCu_2O_7$ (*25, 26*). Thallium can also be partly replaced by bismuth leading to the 1212-type oxides (Tl,Bi) $Sr_2 CaCu_2O_y$ (*27*) and $Tl_{0.5}Bi_{0.5}$, $Ca_{1-x} Y_x$, $Sr_2 CuO_y$ (*28*), which exhibit critical temperatures ranging from 83 to 102 K.

The "1223"-phase $TlBa_2Ca_2Cu_3O_9$, whose structure involves triple copper layers with copper in pyramidal and square planar coordination (Fig. 8b), was isolated at the beginning of 1988 (*29, 30*) and confirmed several months later by different authors (*31*). Contrary to the 1212-type oxides, the critical temperature of this phase is not very sensitive to the experimental method of synthesis. The replacement of thallium by lead in the thallium monolayers is also possible and allows the strontium cuprate $Tl_{0.5}Pb_{0.5} Sr_2Ca_2Cu_3O_9$ (*19*) to be synthesized, whose T_c is also close to 120 K.

The "2212" thallium cuprate $Tl_2Ba_2Ca Cu_2O_8$ (*32–36*) represents the [3,2] member of the series, characterized by thallium bilayers sandwiched by barium layers, the pyramidal copper layers being similar to those observed for the 1212-type oxides (Fig. 8c). Different from $TlBa_2CaCu_2O_7$, this superconductor is easily prepared as a pure phase. At first sight, its critical temperature appears higher than that observed for the "1212" phase. Nevertheless, it should be pointed out that the T_c's observed for this phase varies from one author to the other, ranging from about 97 to 108 K according to the method of synthesis. This latter issue which takes its origin in the oxygen nonstoichiometry will be discussed later. Barium can be replaced by strontium leading to a solid–solution $Tl_2Ba_{2-x}Sr_xCaCu_2O_8$ (*37*) whose T_c curiously decreases from 110 K

for the pure barium phase ($x = 0$) to 44 K for the pure strontium oxide ($x = 2$). The substitution of a lanthanide for calcium in the oxide $Tl_2Ba_2CaCu_2O_8$ has a similar effect to that observed for the "1212" phase; it is indeed observed that in the solid–solution $Tl_2Ba_2Ca_{1-x}Y_xCu_2O_8$, T_c increases with x up to $x = 0.1$ and then decreases dramatically beyond this value. The thallium nonstoichiometry in this phase is in fact very complex. Besides the classical "2212" formula, $Tl_2Ba_2CaCu_2O_8$, isostructural compounds with much richer thallium contents have been isolated corresponding to the formula $Tl_{3-4x/3}Ba_{1+x}LnCu_2O_8$ with Ln = Pr, Nd, Sm and x close to 0.25 (*38*). The structure of one of those oxides $Tl_{2.70}Ba_{1.25}PrCu_2O_8$ clearly shows that a great part of the barium sites are occupied by thallium leading to the formulation $Tl^{III}_{1.95}(Tl^{III}_{0.75}Ba_{1.25})PrCu_2O_8$. Thus, in this oxide the thallium monolayers are approximately unchanged whereas thallium and barium are distributed over the two other layers suggesting that, on those latter sites, thallium exhibits a univalent state. Contrary to the other "2212" oxides this latter phase is not superconductive.

The "2223"-phase $Tl_2Ba_2Ca_2Cu_3O_{10}$ (*32, 34, 35, 39*) represents, up to now, the superconductor which exhibits the highest critical temperature, $T_c \approx 125$ K. Such a structure (Fig. 8d) which consists of triple copper layers as in the "123" phase and triple rock salt layers as in the "2212"-phase has not been synthesized for strontium and in a general manner few substitutions have been successful for this compound. Like the "2212"-phase, this oxide can easily be prepared as a pure phase, i.e., without intergrowths as impurities provided the temperature of the synthesis be controlled carefully. The great difference of this phase with other thallium cuprates, especially with "1212", "2212", "1201", and "2201" oxides, deals with the fact that its critical temperature is not affected by the method of synthesis so that all authors agree with a T_c of 125 K.

One important feature of those thallium cuprates is that the oxygen nonstoichiometry influences drastically their critical temperatures at least for the members corresponding to m smaller than 3. This was indeed shown first for the oxides $TlBa_2CaCu_2O_7$ and $Tl_2Ba_2CuO_6$ (*17*). These latter compounds prepared under oxygen pressure of several atmospheres in sealed ampoules were found to be superconducting ($T_c = 50$ K) and nonsuperconducting, respectively; annealing these samples at 450–500°C under an argon flow allowed T_c to be increased up to 65 K for the first one and superconductivity at 30 K to be obtained for the second one. The fact that the superconducting transition can be increased by decreasing the oxygen content was then confirmed later for $Tl_2Ba_2CuO_6$ (*40, 41*) whereas the opposite was found for $Tl_2Ba_2CaCu_2O_8$ (*42*) and $Tl_2Ba_2Ca_2Cu_3O_{10}$ (*43*). A study of the annealing of $Tl_2Ba_2CaCu_2O_8$ crystals under argon and vacuum (*18*) showed a more complex behavior: for one of the crystals T_c decreased by vacuum annealing, whereas for the others T_c increased significantly. A recent study of $Tl_2Ba_2CaCu_2O_8$ clearly shows that in those cuprates the critical temperature is mainly governed by the oxygen stoichiometry (*44*). Starting from a sample synthesized under an oxygen pressure of about 4–7 bars in sealed tubes three sorts of annealings were performed in a first step corresponding to samples A, B, and C, respectively. For sample A, annealing was performed at 400°C in an oxygen flow. For sample B, annealing was carried out in an argon flow at 400°C. For sample C, the sealed silica ampoule containing the "as-synthesized" sample was cooled down to 400°C and kept at this temperature for 12 hr and then slowly cooled down to room temperature. Figure 9a shows the real part χ' of the AC susceptibility of the A (or B) as-synthesized sample (A and B were synthesized in the same evacuated ampoule) of oxygen annealed sample A and of argon-

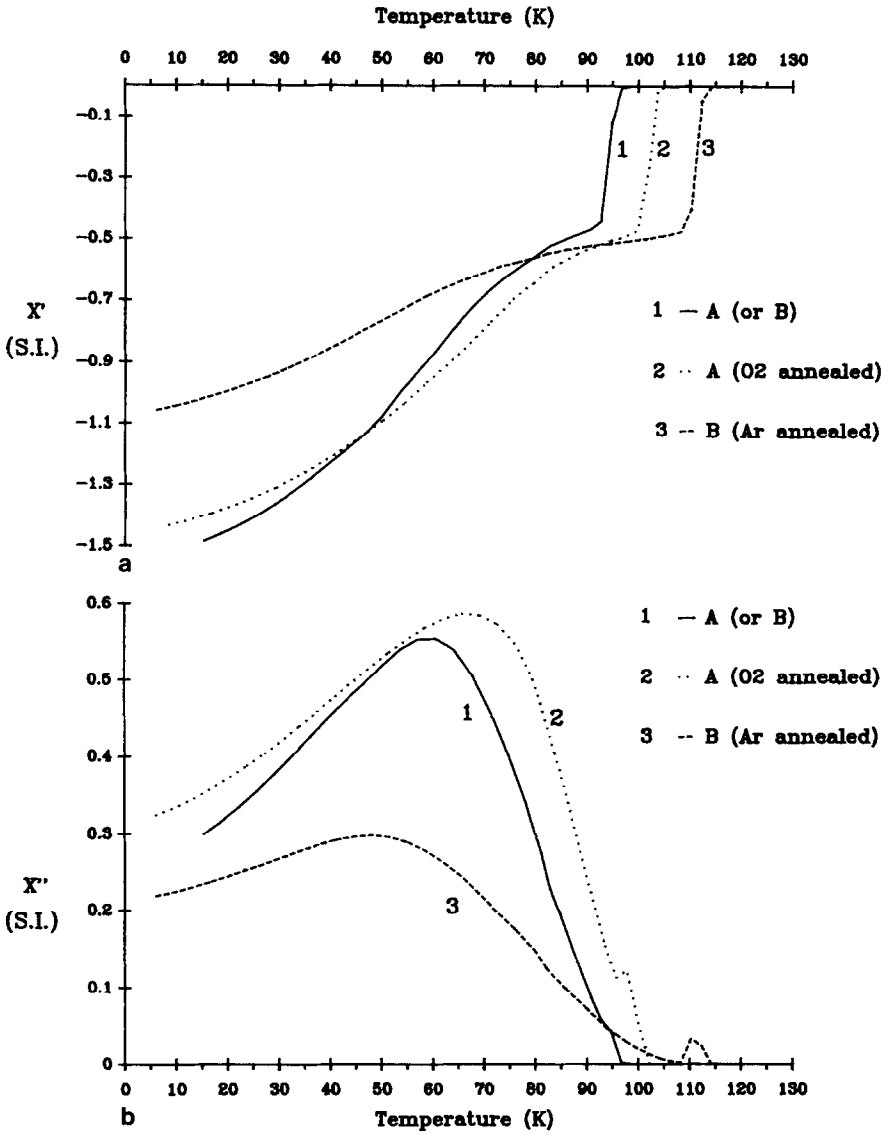

FIG. 9. (a) Real part $\chi'(T)$ of the magnetic AC susceptibility of thallium cuprates $Tl_2Ba_2CaCu_2O_8$: (1) as synthesized sample ($T_c \approx 96$ K), (2) sample annealed under oxygen flow at 400°C, (3) sample annealed under argon flow at 400°C. (b) Imaginary part $\chi''(T)$ of the magnetic AC susceptibility corresponding to the curves in (a).

annealed sample B. The data are not corrected for the demagnetizing effects as shown from the χ' values smaller than -1. The first important result deals with the fact that the critical temperature is increased as well by argon annealing as by oxygen annealing. One indeed observes that T_c is about 97 K for the as-synthesized samples, whereas it is increased up to 104 K by oxygen annealing (sample A) and up to about

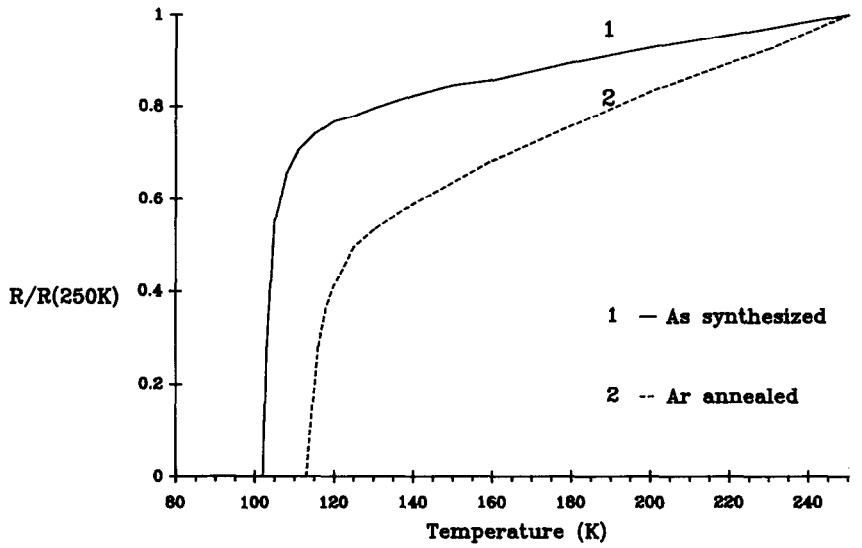

FIG. 10. Electrical resistance versus T for a $Tl_2Ba_2CaCu_2O_8$ sample: (1) as synthesized sample ($T_c \approx$ 100 K), (2) the same sample annealed under argon flow at 400°C.

112 K by argon annealing (sample B). The AC magnetic field amplitude (5 Oe) was the same for the three curves reported in Fig. 9. The difference between the magnetization in the low temperature range comes from the grain decoupling as can be seen on the imaginary part χ'' of the magnetic susceptibility versus temperature (Fig. 9b). These magnetization measurements are confirmed by electrical resistance as can be seen in Fig. 10 for the argon annealing effect on the as-synthesized samples.

At this stage of the experiment it appears that oxygen loss during annealing either under argon or oxygen flow should be responsible for the increase of T_c's, suggesting that it allows the optimal hole carrier density to be reached by those thermal treatments. In order to confirm this hypothesis, sample C ($T_c \sim 98$ K) was heated in an evacuated ampoule in the presence of zirconium turnings for 12 hr at 400°C. The χ' (T) curve after annealing of the C′ sample shows a spectacular increase for the critical temperature (Fig. 11): $\Delta T_c \approx 17$ K. However, the diamagnetic volume of the grains started to decrease, owing to the long annealing time in these conditions. The C′ sample was then heated at 800°C for 1/2 hr in air, and finally rapidly cooled down to room temperature. The resulting C″ sample shows a decrease of T_c down to 105 K (Fig. 11) but the diamagnetic volume in the low temperature range is largely increased compared to C′, showing a good evidence of grain boundaries "reconstruction."

It is clear from these experiments that there exists an optimum of the hole carriers density leading to a maximum of T_c. Nevertheless, although the oxygen nonstoichiometry seems to play an important role in this phenomenon, the weight loss may also result from the thallium oxide volatilization. The volatility of thallium oxide at 400°C was indeed demonstrated for this compound by chemical analysis. In order to avoid this thallium loss the annealing of $Tl_2Ba_2CaCu_2O_8$ was then performed at 300°C in reducing at-

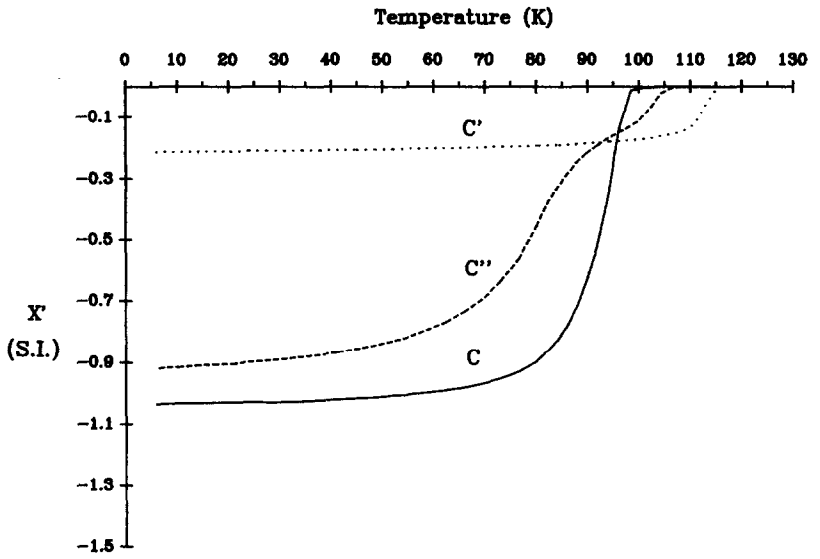

FIG. 11. Real part $\chi'(T)$ of the AC susceptibility of a $Tl_2Ba_2CaCu_2O_8$ sample prepared with the same synthesis conditions as samples A and B (Fig. 9a): (C) sample annealed at 400°C under oxygen pressure in sealed silica ampoule, (C') the same sample annealed in evacuated silica ampoule with Zr turnings at 400°C for 12 hr, (C'') the C' sample heated during 1/2 hr at 800°C in air.

mosphere (argon–hydrogen); under these conditions no thallium loss was observed. A spectacular effect of this method of annealing upon T_c's was observed as shown on Fig. 12. T_c can indeed be increased from 96 to 118 K for a very short annealing time of 15 min. It can also be seen that the variation of the annealing time does not influence drastically the T_c's but that a prolonged annealing tends to decrease the diamagnetic volume. The weight losses determined by TGA corresponding to each of these curves are listed in Table III. It is worth pointing out that the weight losses are very small, and that the smallest weight loss of 0.07% leads to a dramatic increase of T_c's: $\Delta T_c \approx 22$ K.

Similar effects were observed for the "1212" phase $TlBa_2CaCu_2O_7$ and for $Tl_2Ba_2CuO_6$ whose study is in progress (*47*), whereas the influence of this annealing is considerably decreased as the number m of copper layers increases; the critical temperature of $TlBa_2Ca_2Cu_3O_9$ is only increased of 5 K, whereas for $Tl_2Ba_2Ca_2Cu_3O_{10}$ T_c remains unchanged (125 K). It must also be emphasized, from the HREM observations, that the treatment under hydrogen at 300°C does not alter the materials, contrary to the annealings at 400–500°C under different atmospheres. The oxygen nonstoichiometry is the key for the optimization of the superconducting properties and especially the critical temperature of the thallium cuprates, owing to its great influence upon the hole carrier density. This explains why the values of T_c observed for the "2212" phase could be rather different from one author to the other, depending upon the oxygen pressure and temperature and time used for its preparation (*18, 45–46*).

It is worth pointing out that the effect of oxygen nonstoichiometry upon T_c's is all the more important since the number of copper

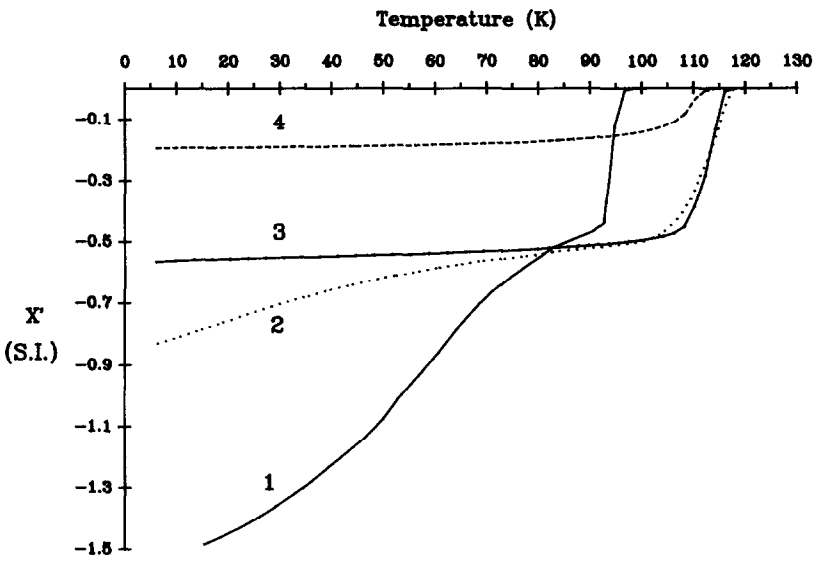

FIG. 12. AC susceptibilities $\chi'(T)$ of the same sample Tl"2212" for different annealing times in a gas mixture (Ar 90% + H_2 10%). Annealing times and weight losses are listed in Table III.

layers forming the perovskite slabs is smaller, i.e., since m is smaller. One indeed observes ΔT_c variations of 90 K for $Tl_2Ba_2CuO_6$ ($m = 1$), of more than 20 K for $TlBa_2CaCu_2O_7$ and $Tl_2Ba_2CaCu_2O_8$ ($m = 2$), and of 0–5 K for $TlBa_2Ca_2Cu_3O_9$ and $Tl_2Ba_2Ca_2Cu_3O_{10}$ ($m = 3$). Thus, the important factor which governs the T_c's in thallium cuprates is the hole carrier density per mole of copper in the structure (equivalent to the number of Cu(III) per mole Cu) and this factor seems to be predominant with respect to the effect of the number m of copper layers in the perovskite slabs.

The main issue which remains to be solved deals with the knowledge of oxygen content and distribution in the structure, and consequently the actual carrier density. Nevertheless the "annealing at 300° in a reducing atmosphere" appears as a very powerful

TABLE III

EFFECT OF ANNEALING IN AN Ar/H_2 FLOW AT 300°C UPON SUPERCONDUCTING PROPERTIES OF $Tl_2Ba_2CaCu_2O_8$

"2212" Sample	Annealing period	Total weight loss	T_c (K)
1	Untreated		96
2	15 min	0.07%	118
3	120 min	0.4%	117
4	720 min	2.2%	115

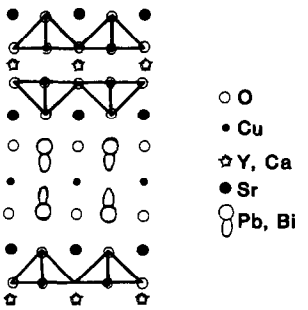

FIG. 13. Schematized [110] projection of the structure of $Sr_2(Pb,Bi)_2Ca_{1-x}Y_xCu_3O_8$.

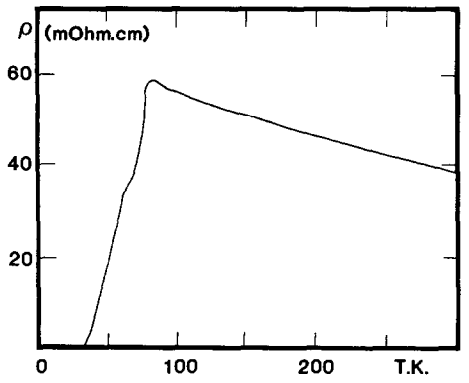

FIG. 14. Resistivity versus temperature for a polycrystalline sample of $Pb_2Sr_2(Ca,Y)Cu_3O_8$ from Cava *et al.* (*48*).

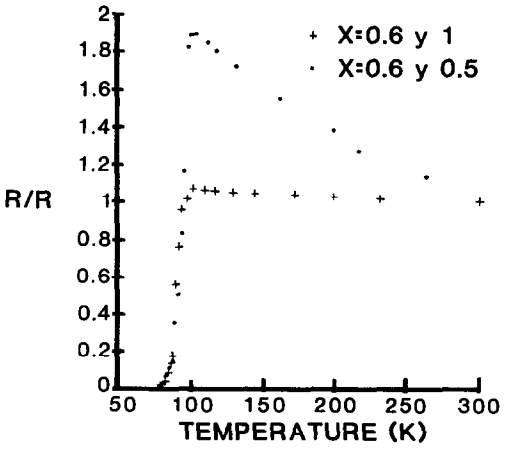

FIG. 15. Resistance normalized to $R_{300\,K}$ versus temperature for the oxides $Pb_{2-x}Bi_xSr_2Ca_yY_{1-y}Cu_3O_8$: $x = 0.6$, $y = 1$ and $x = 0.6$, $y = 0.5$.

method to control the hole carrier density and consequently, the T_c's of those cuprates without altering the structure.

III. Superconductive Lead Cuprates: Promising Materials but Broad Resistive Transitions

Among the different layered cuprates only three series of lead oxides are characterized by double and triple copper layers:

—The $BaPbYSrCu_3O_8$ series (*11*).

—The $Pb_2Sr_2Ca_{1-x}Y_xCu_3O_8$ series (*48, 49*).

—The $Pb_{0.5}Sr_{2.5}Ca_{1-x}Y_xCu_2O_{7-\delta}$ series (50–52).

$BaPbYSrCu_3O_8$ (*11*) is the only "pure lead" cuprate with triple copper layers, but unfortunately is not superconductor as already discussed above.

The superconductor $Pb_2Sr_2Ca_{1-x}Y_xCu_3O_8$ discovered by Cava *et al.* (*48*) is formed of copper bilayers. Its structure (Fig. 13) consists of double pyramidal copper layers alternatively with single copper layers so that it can be described as a double intergrowth of double and single deficient perovskite layers with single rock salt-type layers.

In fact, this material is characterized like $YBa_2Cu_3O_{7-\delta}$ with $\delta > 0$, by a disproportionation of Cu(II) into Cu(III) and Cu(I) (*53*) so that the single copper layers are only formed of Cu^IO_2 rods involving univalent copper whereas the double pyramidal layers exhibit the mixed valency Cu(II)–Cu(III). It is most probable that superconductivity takes its origin in those latter double copper

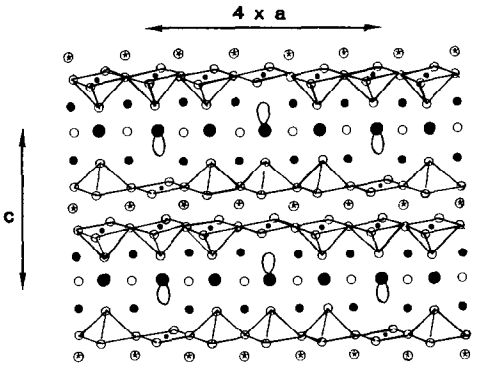

FIG. 16. $Pb_{0.5}Sr_{2.5}Y_{1-x}Ca_xCu_2O_{7-\delta}$: model of a perfect ordering of the Pb(II) and Sr in the intermediate rock salt layers. This idealized drawing shows that $4a \times c$ superstructure can be built up. Other models can be obtained by translation of the adjacent layers.

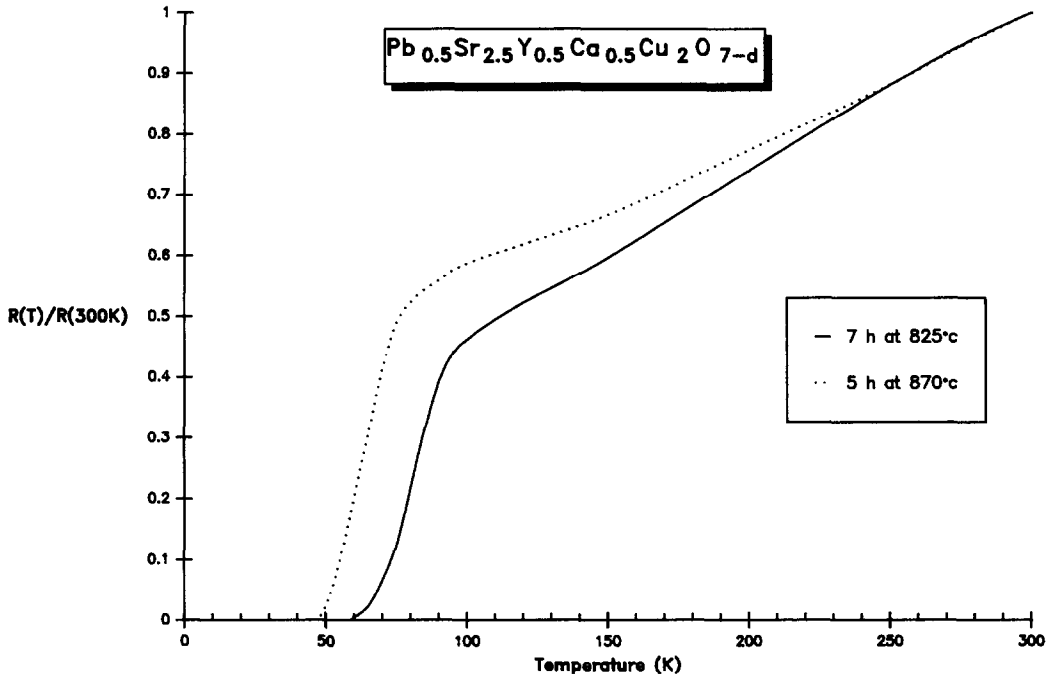

FIG. 17. Temperature dependence of the ratio $R(T)/R(300\ K)$ for different synthesis conditions (unannealed samples) for $Pb_{0.5}Sr_{2.5}Y_{1-x}Ca_xCu_2O_{7-\delta}$.

layers. it must be emphasized that the synthesis of this oxide, which is performed under a reduced oxygen pressure, is difficult. Moreover the resistive transition is very broad with a T_c (onset) of 80 K and T_c offset of 46 K (Fig. 14). The substitution of bismuth for lead allows the superconducting properties of this phase to be considerably improved. The critical temperature of the isostructural oxides $Pb_{2-x}Bi_xSr_2Y_{1-y}Ca_yCu_3O_8$ (*49*) is indeed displaced towards higher values as shown for instance for $Pb_{1.40}Bi_{0.60}Sr_2Y_{0.50}Ca_{0.50}Cu_3O_8$ which exhibits a T_c (onset) of 100 K and a zero resistance at 79 K (Fig. 15). But here again the resistive transition remains broad and could not be improved up to now.

The oxide $Pb_{0.5}Sr_{2.5}Y_{1-x}Ca_xCu_2O_{7-\delta}$ (*50, 51*) is the only pure lead cuprate which exhibits double copper layers. Its structure (Fig. 16) belongs indeed to the "1212"-type already described for $TlA_2\ CaCu_2O_7$ (A = Ba,Sr) (Fig. 8a). Mixed lead–strontium monolayers $[Pb_{0.5}Sr_{0.5}O]_\infty$ replace the $[TlO]_\infty$ monolayers in the double rock salt slabs. Nevertheless an important difference with the thallium cuprates deals with the existence of oxygen vacancies at the boundary between the perovskite and rock salt-type layers. It results in the existence of several superstructures which can be interpreted in terms of ordering of lead, strontium, and anionic vacancies. An isostructural solid–solution has been isolated by replacing completely strontium by calcium in the mixed monolayers leading to the formation $Pb_{0.50}Ca_{0.50}Sr_2\ Y_{1-x}Ca_xCu_2O_{7-\delta}$ (*52*). Both oxides exhibit a wide homogeneity range, $0 \leq x \leq 0.60$, but curiously superconductivity is only observed for $0.50 \leq x \leq 0.60$.

In all cases, one again observes very broad resistive transitions as shown for in-

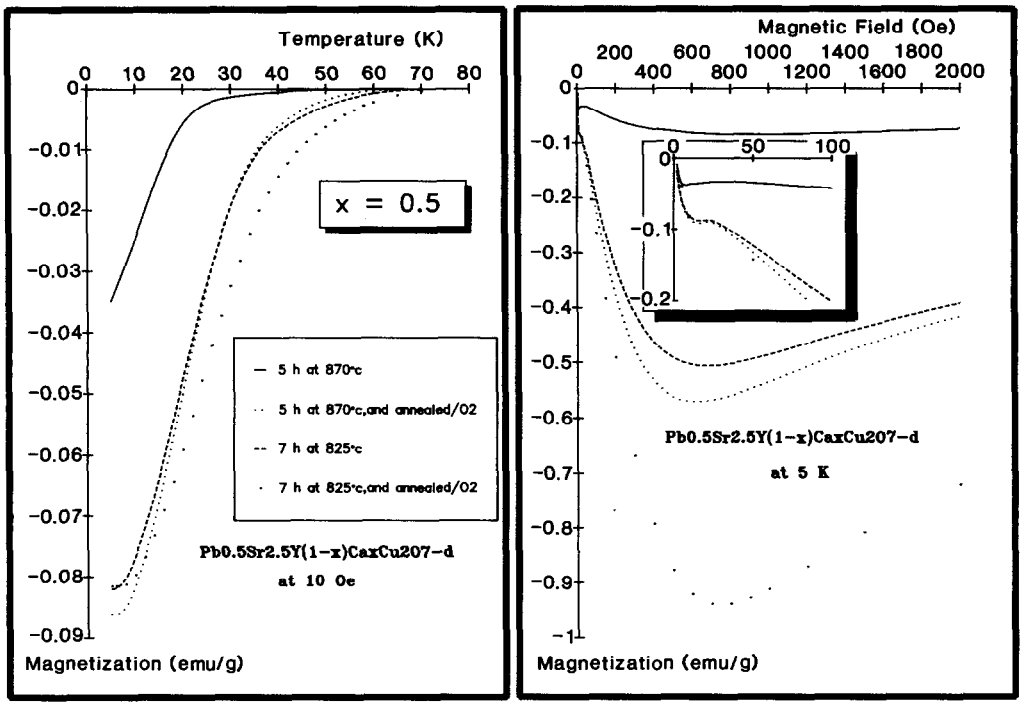

FIG. 18. (a) Magnetization vs T for $Pb_{0.5}Sr_{2.5}Y_{1-x}Ca_xCu_2O_{7-\delta}$ ($x = 0.5$) at 10 Oe for different thermal treatments, (b) magnetization vs H($H < 2000$ Oe) at 5 K for the same samples. Insert shows the low field part of the curves.

stance for $Pb_{0.5}Sr_{2.50}Y_{0.50}Ca_{0.5}Cu_2O_{7-\delta}$ (Fig. 17). Moreover, it can be seen that the experimental conditions, especially the temperature, influence dramatically the superconducting properties of those materials. This behavior is confirmed by the magnetic study performed with a SQUID magnetometer (Fig. 18). For instance, one observes that annealing under an oxygen flow at about 500°C increases T_c (onset) from 60 to 70 K, and that, in the same way, synthesis performed at 825°C led to much better results than at 870°C. An interesting feature deals with the compositions corresponding to x greater than 0.60 which are not single phased, but which present superconductivity at higher temperature. This is indeed the case of the composition "$x = 0.90$" which presents a diamagnetic signal corresponding to 3–4% of the sample volume and a T_c of 104 K (Fig. 19); of course, for this latter composition, zero resistance cannot be reached, owing to the large volume of the insulating phase belonging to the Sr_2PbO_4-type which prevents the percolation. Nevertheless, this confirms the possibility of superconductivity up to 100 K in those systems, and suggests the possible existence of another superconductive lead cuprate.

Although it is not the purpose of this review, the HREM study of these materials must be emphasized here, since it shows the great flexibility of the structure, suggesting the possibility to synthesize new structural types. For instance, the exploration of the oxide $Pb_{1.4}Bi_{0.6}Sr_2Y_{0.5}Ca_{0.5}Cu_3O_8$ (*54*) evidenced an antiphase boundary oriented at 45° with respect to $\vec{c}$ (Fig. 20a) which could be interpreted by the structural model given in Fig. 20; in this model across the bound-

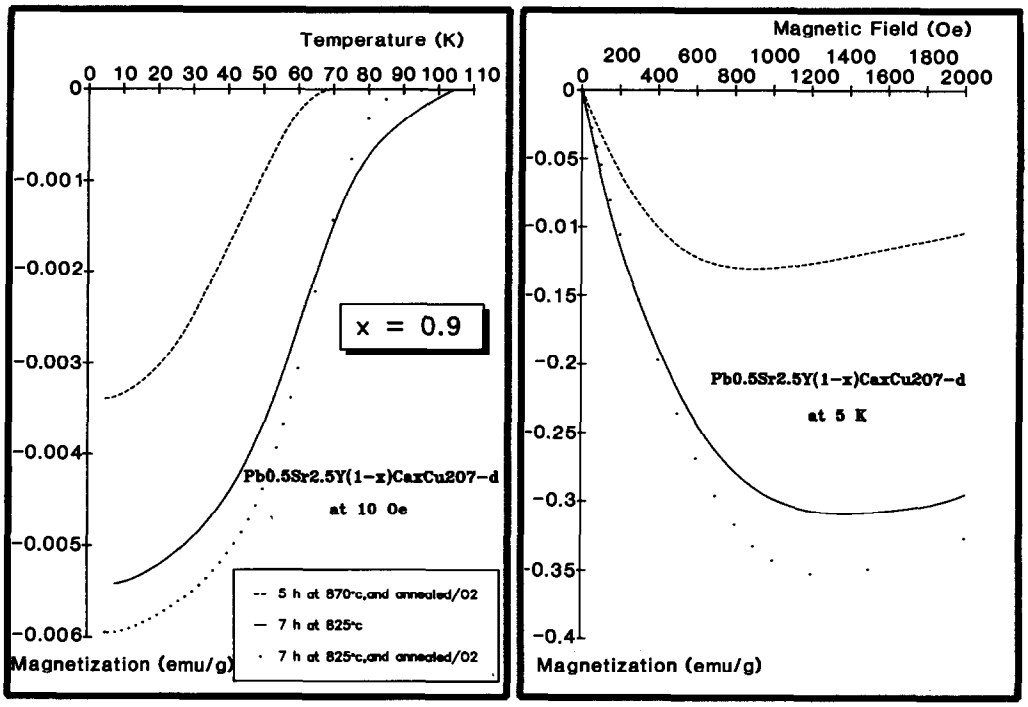

FIG. 19. Multiphase sample of nominal composition $Pb_{0.5}Sr_{2.5}Y_{1-x}Ca_xCu_2O_{7-\delta}$ ($x = 0.9$): (a) Magnetization vs T at 10 Oe for different thermal treatments, (b) magnetization vs H($H < 2000$ Oe) at 5 K.

ary, the $[SrO]_\infty$ layers remain unchanged whereas the $[CuO_2]_\infty$ layers are connected to the $[PbO]_\infty$ layers. Another example was also often observed in that oxide, with an antiphase boundary almost parallel to (110) (Fig. 21a). The idealized model (Fig. 21b) proposed for this extended defect shows that the antiphase boundary appears in (AO) plane (A = Sr, Ca, or Y); it can be seen that two types of layers are unchanged, one $[CuO_2]_\infty$ and one $[PbO]_\infty$ layer out of two, whereas the second $[CuO_2]_\infty$ and $[PbO]_\infty$ are connected through the boundary.

Thus, the layered cuprates form a potential family of high T_c superconductors. However, their crystal chemistry is complicated by the two possible states Pb(II)/Pb(IV), which are also important species for the creation of new superconductors. A systematic study of the oxygen nonstoichiometry in these oxides will be necessary to control their synthesis and to improve the oxygen homogeneity in the crystal.

IV. The Bismuth Cuprates: Reversibility and Proximity Effects

Although rather similar to the thallium copper system the crystal chemistry of the bismuth cuprates is less rich than that of thallium. Only two series of oxides have indeed been synthesized, both characterized by triple rock salt-type layers built up from bismuth bilayers sandwiched by SrO layers. Thus, the existence of bismuth bilayers seems absolutely necessary to stabilize such structures.

The 85 K superconductor $Bi_2Sr_2CaCu_2O_8$ (*55–63*) belongs to the 2212 series, i.e., has its structure (Fig. 8b) similar to that of the

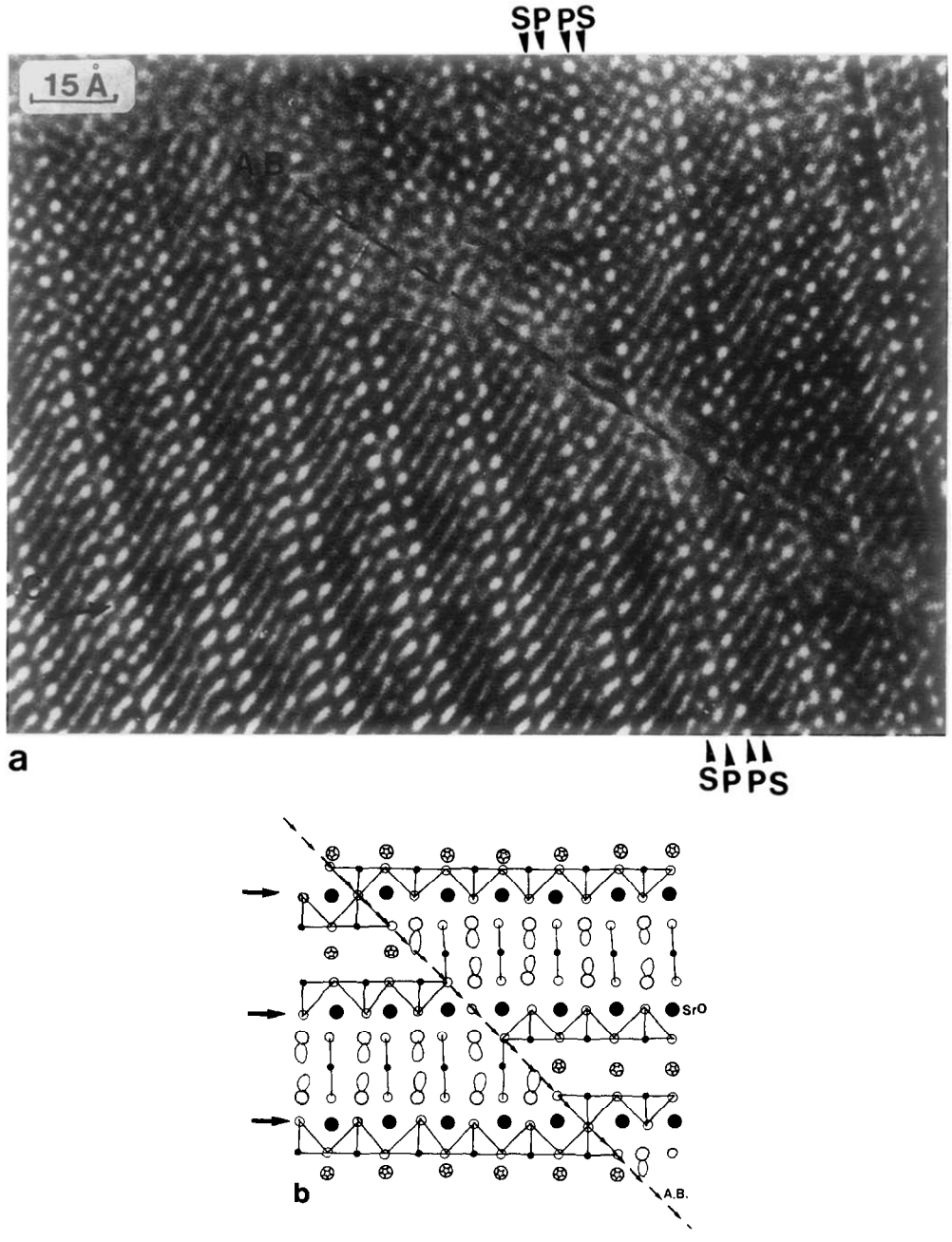

FIG. 20. $Pb_{1.4}Bi_{0.6}Sr_2Ca_{0.5}Y_{0.5}Cu_3O_8$: (a) [110] HREM image of a 45° antiphase boundary (AB). The nature of the cationic strontium and lead layers is indicated as S and P, respectively; the boundary is outlined by a row of small black arrows. (b) Idealized drawing of the connection of the different layers through the 45° antiphase boundary. The SrO layers which remain unchanged through the boundary are shown with large black arrows. The 45° boundary is parallel to an oxygen plane (row of small arrows).

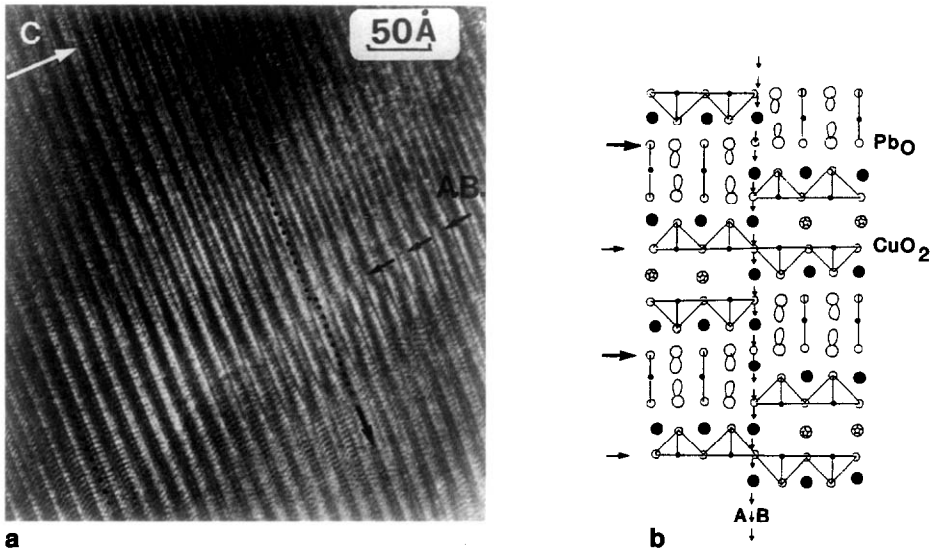

FIG. 21. $Pb_{1.4}Bi_{0.6}Sr_2Ca_{0.5}Y_{0.5}Cu_3O_8$: (a) [110] image of an antiphase boundary parallel to the $\vec{c}$ axis in the thick part of the crystal. The shifting of the layers through the boundary is close to $c/4$ (indicated by rows of small dots parallel to the layers). (b) Idealized drawing of the connection of the layers through the antiphase boundary parallel to (110). The unchanged planes, [PbO] and [CuO], are indicated by large and medium arrows. The boundary appears in an AO plane (rows of small arrows).

$Tl_2Ba_2CaCu_2O_8$, the bismuth bilayers replacing the thallium bilayers. Lead can be substituted for bismuth in a wide range without decreasing T_c's as shown for instance for the solid–solution $Bi_{2-x}Pb_xSr_2Ca_{1-x}Y_xCu_2O_8$ (*64*, *65*).

The 108 K superconductor $Bi_2Sr_2Ca_2Cu_3O_{10}$ detected for the first time by Tarascon *et al.* (*66*) is difficult to synthesize as a pure phase (*66–71*). It can be stabilized by lead substitution on the bismuth sites, as shown by Endo *et al.* (*67*), for the phase $Bi_{1.6}Pb_{0.4}Sr_{1.6}Ca_{2.4}O_{10}$. Its structure (Fig. 8d) belongs to the "2223" series, i.e., consists of triple copper layers.

From the structural point of view, these oxides differ from the thallium cuprates by the lamellar character of their structure and by the systematical existence of satellites on E.D. patterns in incommensurate positions. This latter feature which is connected with the waving of the rock salt-type layers has been the subject of many publications (see, for review, Ref. (*72*)). Although of great interest it will not be discussed here. Nevertheless, it must be emphasized that several issues concerning the origin of incommensurability, such as the role of the $6s^2$ lone pair of Bi(III) or the excess oxygen with respect to the ideal formula, are still not clear.

As in the other superconductive cuprates, the superconducting properties of the bismuth cuprates are sensitive to the gazeous atmosphere used for the synthesis. The best results are generally observed for preparation in air, whereas annealing in an oxygen flow tends to kill superconductivity. Very sharp transitions can be obtained like for thallium cuprates.

An important difference of the bismuth cuprates with other superconductive cuprates and especially with respect to $YBa_2Cu_3O_7$ deals with the disappearance of critical currents at very low magnetic fields due to the flux flow phenomenon. In a recent study of the lead doped "2223"-cuprate, De

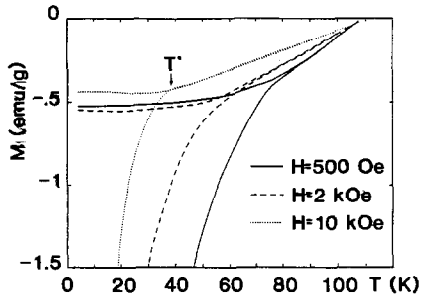

FIG. 22. $Bi_{2-x}Pb_xSr_2Ca_2Cu_3O_{10}$: magnetization vs temperature in different applied fields. Note the linear variation of M vs T in the reversible region and the abrupt change of the slope at T^*.

Rango *et al.* (*73*) have shown from the magnetization measurements versus temperature at different fields (Fig. 22) that the diamagnetism below T^* increased dramatically suggesting a phase transition from a normal to a superconducting state. But the main experimental point observed by these authors deals with the experimental decrease of the irreversibility line which they have fitted with the equation $H^* = 147\,000\, e^{-T/13.3}$ (Fig. 23). This phenomenon was interpreted as the result of a breakdown field in which superconductivity induced by a proximity effect is destroyed. Thus, the layered

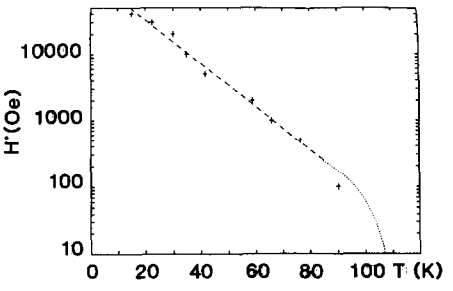

FIG. 23. $Bi_{2-x}Pb_xSr_2Ca_2Cu_3O_{10}$: irreversibility line. The data (+) correspond to the temperature T^* below which a strong increase of the zero field magnetization is observed in different applied fields H. Note the exponential decrease of H^* vs T: $H^* = 147\,000\, e^{-T/13.3}$. Near T_c, H^* has been extrapolated with a $(1 - T/T_c)^{3/2}$ law (dotted line).

cuprates should be considered as a stacking of superconductive copper oxygen layers with normal rock salt layers. However, superconductivity would be induced in the normal layers by proximity effects, leading to a "three-dimensional superconductivity," which would be destroyed by applying a magnetic field. This implies that the "normal" rock salt layers should exhibit a metallic character. The recent X-ray absorption study of those oxides at BiL_{III}-edge (*74*) supports this point of view. One indeed observes a significant shifting at Bi L_{III} edge of the curves of the superconductive cuprates toward lower energy with respect to the curves of Bi_2O_3, or of the isostructural oxide $Bi_2Sr_2CaFe_2O_9$. Such a feature suggests that bismuth exhibits a formal oxidation state intermediate between that of Bi(III) and metallic bismuth which has never been observed up to now in bismuth oxides. This phenomenon can be interpreted by a semimetallic character of the "Bi–O" layers which would result from a narrow band built from the overlapping hybridized s–p bismuth orbitals with $2p$ oxygen orbital. In this model, electrons would be transfered from the copper layers in this conduction band leading to the mixed valency Cu(II)–Cu(III).

Note added in proof. Some days before receiving the proofreading galleys of this paper, superconductivity was definitely observed in the oxides $La_{1.6}Sr_{0.4}CaCu_2O_6$ (5) and $PbBaSrY_{0.7}Ca_{0.3}Cu_3O_8Cu_2O_6$ (76) with a critical temperature of 60 K and 75 K respectively, confirming that the two factors which govern superconductivity in copper oxides remain up to now to dimensionality of the structure and mixed valency of copper as previously stated (77).

References

1. N. NGUYEN, L. ER RAKHO, C. MICHEL, J. CHOISNET, AND B. RAVEAU, *Mater. Res. Bull.* **15**, 891 (1980).

2. F. IZUMI, E. TAKAYAMA-MUROMACHI, Y. NAKAI, AND H. ASANO, *Physica C* **157,** 89 (1989).
3. V. CAIGNAERT, N. NGUYEN, AND B. RAVEAU, *Mater. Res. Bull.* in press (1990).
4. N. NGUYEN, C. MICHEL, F. STUDER, AND B. RAVEAU, *Mater. Chem.* **7,** 413 (1982).
5. N. NGUYEN, J. CHOISNET, AND B. RAVEAU, *Mater. Res. Bull.* **17,** 567 (1982).
6. D. M. DE LEEUW, C. A. H. A. MUTSAERS, G. P. J. GEELEN, AND C. LANGEREIS, *J. Solid State Chem.* **80,** 276 (1989).
7. V. CAIGNAERT, R. RETOUX, M. HERVIEU, C. MICHEL, AND B. RAVEAU, *Physica C,* **167,** 483 (1990).
8. J. J. CAPPONI, C. CHAILLOUT, A. W. HEWATT, P. LEJAY, M. MAREZIO, N. NGUYEN, B. RAVEAU, J. L. THOLENCE, AND R. TOURNIER, *Europhys. Lett.* **3,** 1301 (1987).
9. R. A. STEEMAN, D. M. DE LEEUW, G. P. J. GEELEN, AND E. FRIKKEE, *Physica C* **162–164,** 542 (1989).
10. V. CAIGNAERT, R. RETOUX, C. MICHEL, M. HERVIEU, AND B. RAVEAU, *Physica C,* in press.
11. T. ROUILLON, R. RETOUX, D. GROULT, C. MICHEL, M. HERVIEU, J. PROVOST, AND B. RAVEAU, *J. Solid State Chem.* **78,** 322 (1989).
12. N. NGUYEN, J. CHOISNET, M. HERVIEU, AND B. RAVEAU, *J. Solid State Chem.* **39,** 120 (1981).
13. J. C. BEDNORZ AND K. A. MULLER, *Z. Phys. B* **64,** 189 (1986).
14. Z. Z. SHENG AND A. M. HERMANN, *Nature (London)* **332,** 55 (1988).
15. Z. Z. SHENG AND A. M. HERMANN, *Nature (London)* **332,** 138 (1988).
16. S. S. P. PARKIN, V. F. LEE, A. I. NAZZAL, R. SAVOY, T. C. HUANG, G. GORMAN, AND R. BEYERS, *Phys. Rev. B* **38,** 6531 (1988).
17. M. HERVIEU, A. MAIGNAN, C. MARTIN, C. MICHEL, J. PROVOST, AND B. RAVEAU, *J. Solid State Chem.* **75,** 213 (1988).
18. B. MOROSIN, R. J. BANGHMAN, D. S. GINLEY, J. E. SCHIRBERAND, AND E. L. VENTURINI, *Physica C* **161,** 115 (1990).
19. M. A. SUBRAMANIAN, C. C. TORARDI, J. GOPALAKRISHNAN, P. L. GAI, J. C. CALABRESE, T. R. ASKEW, R. B. FLIPPEN, AND A. W. SLEIGHT, *Science* **242,** 249 (1988).
20. C. MARTIN, J. PROVOST, D. BOURGAULT, B. DOMENGES, C. MICHEL, M. HERVIEU, AND B. RAVEAU, *Physica C* **157,** 460 (1989).
21. F. STUDER, D. BOURGAULT, C. MARTIN, R. RETOUX, C. MICHEL, AND B. RAVEAU, *Physica C* **159,** 609 (1989).
22. C. MARTIN, D. BOURGAULT, C. MICHEL, M. HERVIEU, AND B. RAVEAU, *Mod. Phys. Lett., B* **3,** 93 (1989).
23. A. K. GANGULI, R. NAGARAJAN, K. S. NANJUN DASWAMY, AND C. N. R. RAO, *Mater. Res. Bull.* **24,** 103 (1989).
24. S. NAKAJIMA, M. KIKUCHI, N. KOBAYASHI, H. IWASAKI, D. SHINDO, Y. SYONO, AND Y. MATO, Superconductivity 2nd Int. Symp. on, Nov. 14–17, Tskuba, Ibaraki, Japan, 1989.
25. C. N. R. RAO, A. K. GANGULI, AND R. VIJAYARAGHAVAN, *Phys. Rev. B* **40,** 2565 (1989).
26. R. VIJAYARAGHAVAN, A. K. GANGULI, N. Y. VASANTHACHARYA, M. K. RAJUMON, G. V. KULKARNI, G. SANKAR, D. SARMA, A. K. SOOD, N. CHANDRABHAS, AND C. N. R. RAO, *Supercond. Sci. Technol.* **2,** 195 (1989).
27. S. LI AND M. GREENBLATT, *Physica C* **157,** 365 (1989).
28. Y. T. HUANG, R. S. LIU, N. W. WANG, AND P. T. WU, *Japan. J. Appl. Phys.* **28,** L 1514 (1989).
29. C. MARTIN, C. MICHEL, A. MAIGNAN, M. HERVIEU, AND B. RAVEAU, *C. R. Acad. Sci.* **307,** 27 (1988).
30. S. S. P. PARKIN, V. Y. LEE, A. I. NAZZAL, R. SAVOY, R. BEYERS, AND S. J. LA PLACA, *Phys. Rev. Lett.* **61,** 750 (1988).
31. B. MOROSIN, D. S. GINLEY, J. E. SCHIRBER, AND E. L. VENTURINI, *Physica C* **152,** 587 (1988).
32. R. M. HAZEN, D. W. FINGER, R. J. ANGEL, C. T. PREWITT, N. L. ROSS, C. G. ADIDIACOS, P. J. HEANEY, D. R. VEBLEN, Z. Z. SHENG, A. EL ALI, AND A. M. HERMANN, *Phys. Rev. Lett.* **60,** 1657 (1988).
33. M. A. SUBRAMANIAN, J. C. CALABRESE, C. C. TORARDI, J. GOPALAKRISHNAN, T. R. ASKEW, R. B. FLIPPEN, K. J. MORRISSEY, U. CHOWDHRY, AND A. W. SLEIGHT, *Nature (London)* **332,** 420 (1988).
34. S. S. P. PARKIN, V. Y. LEE, E. M. ENGLER, A. I. NAZZAL, T. C. HUANG, G. GORMAN, R. SAVOY, AND R. BEYERS, *Phys. Rev. Lett.* **60,** 1539 (1988).
35. C. POLITIS AND H. LUO, *Mod. Phys. Lett. B* **2,** 793 (1988).
36. A. MAIGNAN, C. MICHEL, M. HERVIEU, C. MARTIN, D. GROULT, AND B. RAVEAU, *Mod. Phys. Lett. B* **2,** 681 (1988).
37. E. A. HAYRI AND M. GREENBLATT, *Physica C* **156,** 775 (1988).
38. D. BOURGAULT, C. MARTIN, C. MICHEL, M. HERVIEU, AND B. RAVEAU, *Physica C* **158,** 511 (1989).
39. C. C. TORARDI, M. A. SUBRAMANIAN, J. C. CALABRESE, J. GROPALAKRISHNAN, T. R. ASKEW, K. J. MORRISSEY, R. B. FLIPPEN, U. CHOWDHRY, AND A. W. SLEIGHT, *Science* **240,** 631 (1988).
40. Y. KUBO, Y. SHIMIKAWA, T. MANAKO, T. SATO, S. IJIMA, T. ICHIHASHI, AND H. IGARASHI, *Physica C* **162–164,** 991 (1989).

41. K. V. RAMANUJACHARY, S. LI, AND M. GREENBLAT, *Physica C* **165,** 377 (1990).
42. I. K. GOPALAKRISHNAN, P. SASTRY, H. RAJAGPAL, A. SAQWEIRA, J. V. YAKHMI, AND R. M. IYER, *Physica C* **159,** 811 (1989).
43. A. SCHILLING, H. R. OTT, AND F. HULLIGER, *Physica C* **157,** 144 (1989).
44. C. MARTIN, A. MAIGNAN, J. PROVOST, C. MICHEL, M. HERVIEU, R. TOURNIER, AND B. RAVEAU, *Physica C,* **168,** 8 (1990).
45. Y. SHIMIKAWA, Y. KUBO, T. MANAKO, T. SATOH, S. IJIMA, T. ICHIASHI, AND H. IGARASHI, *Physica C* **157,** 279 (1989).
46. A. SULPICE, B. GIORDANENGO, R. TOURNIER, M. HERVIEU, A. MAIGNAN, C. MARTIN, C. MICHEL, AND J. PROVOST, *Physica C* **156,** 243 (1988).
47. C. MARTIN, A. MAIGNAN, J. PROVOST, C. MICHEL, M. HERVIEU, AND B. RAVEAU, *Physica C,* submitted for publication.
48. R. J. CAVA, B. BATLOGG, J. J. KRAJEWSKY, L. W. RUPP, L. F. SCHEEMEYER, T. SIEGRIST, R. B. VAN DOVER, P. MARSH, W. F. PECK, P. K. GALLAGHER, S. H. GLARUM, J. H. MARSHALL, R. C. FARROW, J. V. WASZCZAK, R. HULL, AND P. TREVOR, *Nature (London)* **336,** 211 (1988).
49. R. RETOUX, C. MICHEL, M. HERVIEU, AND B. RAVEAU, *Mod. Phys. Lett. B* **3,** 591 (1989).
50. T. ROUILLON, J. PROVOST, M. HERVIEU, D. GROULT, C. MICHEL, AND B. RAVEAU, *Physica C* **159,** 201 (1989).
51. T. ROUILLON, J. PROVOST, M. HERVIEU, D. GROULT, C. MICHEL, AND B. RAVEAU, *J. Solid State Chem.* **84,** 375 (1990).
52. T. ROUILLON, A. MAIGNAN, M. HERVIEU, C. MICHEL, AND B. RAVEAU, *Physica C,* submitted for publication.
53. B. RAVEAU, C. MICHEL, M. HERVIEU, AND J. PROVOST, *Physica C* **153–155,** 3 (1988).
54. M. HERVIEU, V. CAIGNAERT, R. RETOUX, AND B. RAVEAU, *Mater. Sci. Eng.* **6,** 211 (1990).
55. M. MAEDA, Y. TANAKA, M. FUKUTONI, AND T. ASANO, *Japan. J. Appl. Phys. Lett.* **27,** L209 and L548 (1988).
56. R. M. HAZEN, C. T. PREWITT, R. J. ANGEL, N. L. ROSS, L. W. FINGER, C. G. HADIDIACOS, D. R. VEBLEN, P. J. HEANEY, P. H. HOR, R. L. MENG, Y. Y. SUN, Y. Q. WANG, Y. Y. SUE, Z. J. HUANG, L. GAO, J. BECHTOLD, AND C. W. CHU, *Phys. Rev. Lett.* **60,** 1174 (1988).
57. M. A. SUBRAMANIAN, C. C. TORARDI, J. C. CALABRESE, J. GOPALAKRISHNAN, T. R. ASKEW, R. B. FLIPPEN, K. J. MORRISSEY, U. CHOWDHRY, AND A. W. SLEIGHT, *Science* **239,** 1015 (1988).
58. S. A. SUNSHINE, T. SIEGRIST, L. F. SCHNEEMEYER, D. W. MURPHY, R. J. CAVA, B. BATLOGG, R. B. VAN DOVER, R. M. FLEMING, S. H. GLARUM, S. NAKARA, R. FARROW, J. J. KRAJEWSKI, S. M. ZAHURAK, J. V. VASZCZAK, J. H. MARSHALL, P. MARSH, L. W. RUPP, AND W. F. PECK, *Phys. Rev. B* **38,** 893 (1988).
59. J. M. TARASCON, Y. LEPAGE, P. BARDOUX, B. G. BAGLEY, L. H. GREENE, W. R. MC KINNON, G. W. HULL, M. GIROUD, AND D. M. HWANG, *Phys. Rev., B* **37,** 9382 (1988).
60. M. HERVIEU, C. MICHEL, B. DOMENGES, Y. LALIGANT, A. LEBAIL, G. FEREY, AND B. RAVEAU, *Mod. Phys. Lett.* **2,** 491 (1988).
61. P. BORDET, J. J. CAPPONI, C. CHAILLOUT, J. CHEMAVAS, A. W. HEWAT, E. A. HEWAT, J. L. HODEAU, M. MAREZIO, J. L. THOLENCE, AND D. TRANQUI, *Physica C* **153–155,** 623 (1988).
62. T. KAJITANI, K. KUSABA, M. KIBUCHI, N. KOBAYASHI, Y. SYONO, T. B. WILLIAMS, AND M. HIRABAYASHI, *Japan. J. Appl. Phys. Lett.* **27,** L587 (1988).
63. H. G. VON SCHNERING, L. WALZ, M. SCHWARTZ, W. BEKER, M. HARTWEG, T. POPP, B. HETTLICH, P. MÜLLER, AND G. KÄMPF, *Angew, Chem.* **27,** 574 (1988).
64. R. RETOUX, V. CAIGNAERT, J. PROVOST, C. MICHEL, M. HERVIEU, AND B. RAVEAU, *J. Solid State Chem.* **79,** 157 (1989).
65. A. ONO, *Japan. J. Appl. Phys.* **28,** L493 (1989).
66. J. M. TARASCON, Y. LE PAGE, L. H. GREENE, B. G. BAGLEY, P. BARBOUX, D. M. HWANG, G. W. HULL, W. R. MCKINNON, AND M. GIROUD, *Phys. Rev., B* **38,** 2504 (1989).
67. U. ENDO., S. KOYAMA, AND T. KAWAI, *Japan. J. Appl. Phys. Lett.* **27,** L1476 (1988).
68. S. KEMMLER-SACK, A. EHMANN, R. KIEMEL, S. LOSCH, W. SCHAFER, L. KAN, AND B. ELSCHNER, *J. Less-Common Met.* **144,** L1 (1988).
69. J. M. TARASCON, W. R. MCKINNON, P. BARBOUX, D. M. HWANG, B. G. BAGLEY, L. H. GREENE, G. W. HULL, Y. LE PAGE, N. STOFFEL, AND M. GIROUD, *Phys. Rev. B* **38,** 8885 (1988).
70. N. KIJIMA, H. ENDO, J. TSUCHIYA, A. SUMIYAMA, M. MIZUMO, AND Y. OGURI, *Japan. J. Appl. Phys. Lett.* **27,** L1852 (1988).
71. P. LEJAY, P. DE RANGO, A. SULPICE, B. GIORDANENGO, R. TOURNIER, R. RETOUX, F. DESLANDES, C. MICHEL, M. HERVIEU, AND B. RAVEAU, *Rev. Phys. Appl.* **24,** 485 (1989).
72. C. MICHEL, C. MARTIN, M. HERVIEU, D. GROULT, D. BOURGAULT, J. PROVOST, AND B. RAVEAU, Proc. Int. Symp. Superconductivity, Hsinchu, Taiwan, April 1989.
73. P. DE RANGO, B. GIORDANENGO, R. TOURNIER, A. SULPICE, J. CHAUSSY, G. DEUTSCHER, J. L. GENICON, P. LEJAY, R. RETOUX, AND B. RAVEAU, *J. Phys. Fr.* **50,** 2857 (1989).

74. R. RETOUX, F. STUDER, C. MICHEL, B. RAVEAU, A. FONTAINE, AND E. DARTYGE, *Phys. Rev., B* **41,** 193 (1990).

75. R. J. CAVA, B. BATLOGG, R. B. VAN DOVER, J. J. KRAJEWSKI, J. V. WASZCZAK, R. M. FLEMING, W. F. PECK JR; L. W. RUPPO JR; P. MARSH, A. C. W. P. JAMES, *Nature, (London)* **345,** 602 (1990).

76. A. TOKIWA, M. NAGOSHI, T. OKU, N. KOBAYASHI, M. KIKUCHI, K. HIRAGA, Y. SYONO, *Physica C* **168,** 285 (1990).

77. B. RAVEAU, C. MICHEL, *in* "Novel Superconductivity," (A. Wolf and V. Kresin, Eds.), p. 599. Plenum, New York (1987).